Measuring the geometric component of the transition probability in a two-level system

J. W. Zwanziger

Department of Chemistry, Indiana University, Bloomington, Indiana 47405

S. P. Rucker and G. C. Chingas

Materials and Chemical Sciences Division, Lawrence Berkeley Laboratory, 1 Cyclotron Road, Berkeley, California 94720
and Department of Chemistry, University of California, Berkeley, California 94720
(Received 17 September 1990)

We describe the measurement of a component of the nonadiabatic transition probability in a two-level system that depends only on the path through parameter space followed by the Hamiltonian, and not on how fast the path is traversed [M. V. Berry, Proc. R. Soc. London **430**, 405 (1990)]. We performed the measurement by sweeping a radio-frequency field through the Zeeman resonance of carbon-13 in a static magnetic field and measuring the transition probability P at the end of each sweep. We found that, for appropriately chosen radio-frequency sweep forms, a factor of P is independent of the duration of the sweep, in accordance with the theory of Berry.

I. INTRODUCTION

Recent work has shown that, even in few-level quantum-mechanical systems, analysis by separation into subsystems typically involves effective interactions between the subsystems that are naturally described in terms of gauge fields.[1,2] Such fields arise for subsystems consisting of dynamical variables, as in the Born-Oppenheimer approximation, and when one of the subsystems consists of external parameters. Examples giving rise to Abelian and non-Abelian gauge fields have been treated theoretically and experimentally.[1,2] Abelian gauge fields have been shown to alter the phases of the wave functions they act on; in the adiabatic limit the phases are shifted by Berry phases.[3] Non-Abelian fields alter both phases and populations. In a significant recent development, Berry has shown how a *Berry phase* in a driven two-level system fundamentally changes the *transition probability* in that system.[4] The purpose of the present paper is to report the experimental confirmation of this prediction.

We are concerned in this paper with a unitarily evolving two-level system depending on external parameters that are changing nonadiabatically. Effective Abelian and non-Abelian gauge potentials applicable to nonadiabatic behavior have been discussed from several points of view, both for unitary[5-9] and nonunitary[10-13] evolution; while the non-Abelian theories permit both phase and population changes, these treatments of Abelian fields describe population changes geometrically only in the case of nonunitary evolution. Several authors have also considered geometric effects on the phase of the transition *amplitude* in a unitarily evolving two-level system.[14-16] The recent work of Berry derives a wholly new result: it predicts a geometric component of the transition probability in a unitarily evolving two-level system. This geometric component depends only on the curve followed by the Hamiltonian in its space of parameters, and not on how fast the curve is followed. The transition probability is the product of the geometric factor and a dynamical factor, which is exponentially small in the rate of change of the parameters; thus although the geometric factor is nonzero even in the adiabatic limit, the complete transition probability still goes to zero as the rate of change goes to zero.

In the following section of this paper we briefly outline the theory of Berry, showing its roots in the Landau-Zener and Dykhne formulas for the transition probability in two-level systems in order to fix notation and make our presentation more self-contained. We then discuss how the measurement is carried out, and the experimental significance of the parameters in the theory. In the final sections, results are presented, and we indicate possible future directions and applications for this work.

II. THEORY

Landau-Zener theory provides an exact expression for the nonadiabatic transition probability in a two-level system described by the following Hamiltonian:

$$\hat{H} = \begin{bmatrix} E_0 + \alpha t & E_{12} \\ E_{12} & E_0 - \alpha t \end{bmatrix} , \tag{1}$$

where E_0, E_{12} and α are real, constant parameters, and t is the time.[17,18] This Hamiltonian provides a simple model for a wide variety of phenomena, such as rapid passage experiments in NMR and nonadiabatic processes in atomic and molecular scattering. The instantaneous (adiabatic) eigenvalues of this system are

$$E_{1,2} = E_0 \pm (\alpha^2 t^2 + E_{12}^2)^{1/2} , \tag{2}$$

and thus represent an avoided crossing as t varies from $-\infty$ to ∞. The complete time-dependent wave function for this two-level system can be expressed in terms of the adiabatic eigenvalues and wave functions as follows (in units where $\hbar = 1$):

$$\psi(t)=c_1(t)\exp\left[-i\int_{-\infty}^{t}dt'E_1(t')\right]\phi_1(t)$$

$$+c_2(t)\exp\left[-i\int_{-\infty}^{t}dt'E_2(t')\right]\phi_2(t) \ . \qquad (3)$$

Here $\{\phi_1(t),\phi_2(t)\}$ are the instantaneous eigenfunctions of the Hamiltonian of Eq. (1), and $c_1(t)$ and $c_2(t)$ are complex expansion coefficients. Landau-Zener theory provides an exact expression for the nonadiabatic transition probability P, where

$$P=|\langle\phi_2(+\infty)|\psi(+\infty)\rangle|^2 \ , \qquad (4)$$

assuming the initial condition $c_1(-\infty)=1$, $c_2(-\infty)=0$. Physically, P is the probability of finding the system in state 2, given that it began in state 1 and was transported at a constant rate through the avoided crossing. In terms of the matrix elements of the Hamiltonian of Eq. (1), $P=\exp(-\pi E_{12}^2/\alpha)$. Note that P is exponentially small in α; as the rate of change of the Hamiltonian goes to zero, P goes to zero, in accordance with the adiabatic theorem.

For two-state Hamiltonians with more complicated time-dependence, Landau-Zener theory does not apply. Dykhne showed, however, that in the case of a real two-state Hamiltonian with an avoided crossing a Landau-Zener-like expression for P is valid asymptotically, as the adiabatic limit is approached.[19-21] In Dykhne's solution, time is analytically continued into the complex plane, and although the energy levels of the system do not cross for any real value of time, there can be some complex value of time, which we denote t_c, where they do cross. At this value of time, the energies are complex as well. Near t_c, barring accidental cancellations of the individual matrix elements of the Hamiltonian, the analytic structure of the energy-level splitting is determined by $(t-t_c)^{1/2}$.[22] The double-valued nature of the complex square root gives rise to the transitions in this picture—the eigenvectors are associated with the Riemann sheets of the square root, and can therefore interchange labels as they pass by the crossing point. The complex crossing point nearest the real axis dominates the transition probability as the adiabatic limit is approached; Dykhne shows that P is given asymptotically by

$$P=\exp\left[-\frac{4}{\delta}\operatorname{Im}\int_0^{\tau_c}E_2(\tau)-E_1(\tau)d\tau\right] \ . \qquad (5)$$

In this formula, scaled time, defined by $\tau=\delta t$, is used, where δ measures the adiabaticity, or slowness, of passage. τ_c is the crossing point nearest the real-time axis, and E_1 and E_2 are the (complex) instantaneous energies. This expression for P requires that the matrix elements of the Hamiltonian be analytic in a strip that includes both the real-time axis and τ_c, so that the phase integral may be analytically continued off the real-time axis to the crossing point. Like the Landau-Zener expression, Dykhne's formula for P is exponentially small in the rate of change of $\hat{H}$.

Berry's contribution removes the restriction to real Hamiltonians.[4] He considers the general Hermitian two-state Hamiltonian

$$\hat{H}(\tau)=\begin{bmatrix} Z(\tau) & X(\tau)-iY(\tau) \\ X(\tau)+iY(\tau) & -Z(\tau) \end{bmatrix} \ , \qquad (6)$$

or, in spherical polar coordinates (H,θ,φ),

$$\hat{H}(\tau)=H(\tau)\begin{bmatrix} \cos\theta(\tau) & \sin\theta(\tau)\exp[-i\varphi(\tau)] \\ \sin\theta(\tau)\exp[i\varphi(\tau)] & -\cos\theta(\tau) \end{bmatrix} \ . \qquad (7)$$

The expression for the full wave function, Eq. (3) must be modified in this case by the geometric phase (Berry's phase), since here, unlike in the real case, it is not necessarily possible to globally choose the phase of the basis wave functions to be real.[3] The appropriate wave function is then

$$\psi(t)=c_1(t)\exp\left[-i\int_{-\infty}^{t}dt'E_1(t')\right]\exp(i\gamma_1)\phi_1(t)$$

$$+c_2(t)\exp\left[-i\int_{-\infty}^{t}dt'E_2(t')\right]\exp(i\gamma_2)\phi_2(t) \ . \qquad (8)$$

Here, γ_i is the geometric phase of state i, and can be expressed in terms of a line integral over the path C followed by the parameters X,Y,Z, as $\gamma_i=\int_C\mathbf{A}\cdot d\mathbf{R}$, with $\mathbf{A}=\langle\phi_i|\nabla_{\mathbf{R}}\phi_i\rangle$ and $\mathbf{R}$ the vector of parameters.[3] $\mathbf{A}$ is a vector potential (gauge potential), and in the two-state problem under consideration here it is Abelian: it takes the form of a magnetic monopole vector potential located at the origin of parameter space.[3]

As in the case considered by Dykhne, if the matrix elements of the Hamiltonian of Eq. (6) are sufficiently analytic, an asymptotic expression for $\mathbf{P}$ can be developed, now by analytic continuation of both the energy difference and the geometric phase difference. We quote the result from Berry, in spherical coordinates[4]

$$P=\exp\left[-\frac{4}{\delta}\operatorname{Im}\int_0^{\tau_c}d\tau\,H(\tau)\right]$$

$$\times\exp\left[-2\operatorname{Im}\int_0^{\tau_c}d\tau\frac{d\varphi(\tau)}{d\tau}\cos\theta(\tau)\right] \qquad (9)$$

$$=\exp(-\Gamma_d)\exp(+\Gamma_g) \ . \qquad (10)$$

The first factor, $\exp(-\Gamma_d)$, due to continuation of the energy difference, is the same as Dykhne's formula, and is exponentially small in the adiabaticity parameter. This factor is thus dynamical. The second factor, $\exp(+\Gamma_g)$, is due to continuation of the geometric phase, that is, to the Abelian gauge potential $\mathbf{A}$ defined above, and is independent of the adiabaticity parameter. Γ_g is geometric in that it depends on the shape of the path followed by the Hamiltonian, but is independent of how fast the path is traversed. The geometric term is therefore constant, even under adiabatic evolution; it is multiplied, however, by a term which goes to zero in this limit so the adiabatic theorem is satisfied.[23] Note that the derivation of Γ_g makes no reference to closed paths in parameter space, a feature of earlier work on geometric phases that was important for the unambiguous definition of phase shifts.[1,3]

We close this section by noting that Berry discusses conditions that $\hat{H}$ must satisfy to yield a nonzero Γ_g;[4] we

mention these below as we describe our measurement of the geometric component.

III. EXPERIMENTAL IMPLEMENTATION

A. Generating the Hamiltonian

In order to measure the geometric transition probability $\exp(+\Gamma_g)$ we use a variant of a standard technique in NMR, adiabatic rapid passage[24,25] (ARP). The basic ARP experiment works by sweeping a radio-frequency field slowly through a Zeeman resonance *(adiabatic)* but fast on the time scale of longitudinal relaxation *(rapid)*. This process is described by the Hamiltonian (expressed in frequency units)

$$\hat{H}(t) = -\gamma \mathbf{I} \cdot (\mathbf{B}_0 + \mathbf{B}_{rf})$$

$$= -\omega_0 I_z - 2\omega_1 I_x \cos\varphi(t) , \qquad (11)$$

where γ is the magnetogyric ratio of the nucleus; $\mathbf{B}_0$ is the static magnetic field, taken along z, which determines the Larmor frequency $\omega_0 = \gamma |\mathbf{B}_0|$; $\mathbf{B}_{rf}$ is the radio-frequency (rf) magnetic field, taken in the x direction, with amplitude $2\omega_1/\gamma$ and phase $\varphi(t)$; and I_z and I_x are components of the nuclear spin $\mathbf{I}$. In a frame of reference rotating about z in phase with the applied rf field, the Hamiltonian becomes

$$\hat{H}(t) = \Delta\omega(t) I_z - \omega_1 I_x = \omega_{\text{eff}} \cdot \mathbf{I} . \qquad (12)$$

Here the resonance offset $\Delta\omega(t) = \dot{\varphi}(t) - \omega_0$ and the rf amplitude ω_1 define the components of an effective magnetic field ω_{eff} that has magnitude $|\omega_{\text{eff}}(t)| = [\Delta\omega^2(t) + \omega_1^2]^{1/2}$ and makes an angle with the z axis of $\theta(t) = \arctan[-\omega_1/\Delta\omega(t)]$.[24,25]

For a large, initially positive resonance offset, ω_{eff} begins along the $+z$ axis, decreases in length as it sweeps down to exact resonance along the $+x$ axis (reaching its minimum length ω_1), and then lengthens again to finish along the $-z$ axis. For a sufficiently slow sweep, the magnetization will follow this field and also end up aligned along the $-z$ axis. Faster sweeps leave progressively more magnetization behind, causing incomplete population transfer and residual coherence. For linear sweeps ($\dot{\varphi} \propto t$) such as is shown in Fig. 1(a), the actual population transfer is described exactly by the Landau-Zener formula, because the Hamiltonian shown in Eq. (12) has precisely the form of the Hamiltonian of Eq. (1) in this case.

It turns out that Γ_g is zero for the standard Landau-Zener case. Consideration of the formula for Γ_g shows that it is zero for a Hamiltonian curve that can be rigidly rotated into itself about an axis passing through zero,[4] where by Hamiltonian curve we mean a curve in the space of parameters X, Y, Z (I_x, I_y, I_z in the spin case) and parametrized by τ. A Hamiltonian curve that cannot be so rotated is shown in Fig. 1(b) (and Ref. 4); this is the curve used in our experiment, and represents the Hamiltonian

$$\hat{H}(\tau) = A\tau I_z - \omega_1 I_x \cos B\tau^2 - \omega_1 I_y \sin B\tau^2 . \qquad (13)$$

This Hamiltonian is generated experimentally by independently varying the excitation and detection frequencies. Implicit in the discussion of the simple linear sweep was the idea that the signal would be detected in the instantaneous rotating frame defined by the rf. In fact, the resonance offset term, $\Delta\omega$ or $A\tau$, is defined by the difference between the Larmor frequency ω_0 and the detector frequency ω_{det}; trajectories of ω_{eff} in the xy plane of the rotating frame are generated by a transmitter-detector frequency offset. To generate the Hamiltonian shown in Eq. (13), then, it is necessary to sweep both the detector and the rf frequencies linearly through resonance, while offsetting them in a way that decreases linearly to zero as both pass through the Larmor frequency, and then increases linearly again.

A final complication lies in the time parametrization. Rather than choosing the time interval $(-\infty, \infty)$, we use
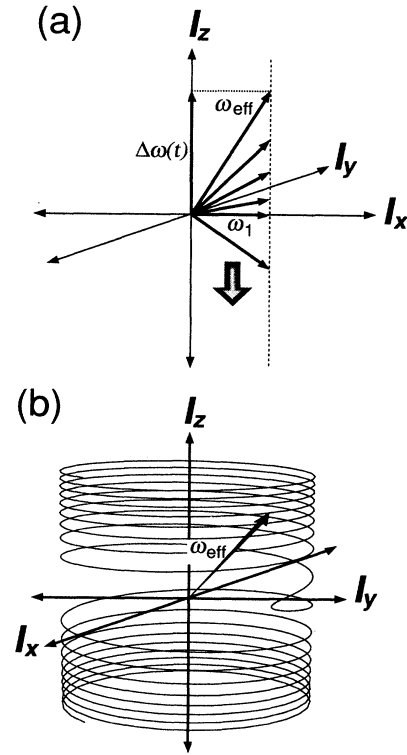

FIG. 1. Hamiltonian curves of the type used in adiabatic rapid passage experiments. The curves are plotted in their three-dimensional parameter space; for NMR experiments these parameters give the orientation of the effective magnetic field ω_{eff} seen by the nuclear spins. The z component of this field is the resonance offset $\Delta\omega = \omega_0 - \omega_{\text{det}}$, where ω_0 is the Larmor frequency and ω_{det} is the detector frequency; the x and y components are $\omega_1 \cos[\int_0^t dt'(\omega_{\text{det}} - \omega_{rf})]$ and $\omega_1 \sin[\int_0^t dt'(\omega_{\text{det}} - \omega_{rf})]$, where ω_1 is the amplitude of the rf field and ω_{rf} its frequency. The adiabaticity parameter δ describes how fast such a curve is traversed, but does not affect its shape in parameter space. Curve (a), a straight line, represents the simple Landau-Zener scenario of Eq. (1); the transition probability for this curve has zero geometric component. Curve (b), the nonuniform helix of Eq. (13), is used in our experiments.

the closed interval $t \in [0, T]$, since our experiments have a definite beginning and end. Then it is natural to use $\delta = 1/T$ as the scale of adiabaticity, and take scaled time in the interval $\tau \in [0,1]$. Finally, we symmetrize the Hamiltonian about the origin of parameter space, giving the final form

$$\hat{H} = 2A(\tau - \tfrac{1}{2})I_z - \omega_1 I_x \cos B(\tau - \tfrac{1}{2})^2$$

$$- \omega_1 I_y \sin B(\tau - \tfrac{1}{2})^2 . \qquad (14)$$

The procedure used to generate this Hamiltonian is illustrated in Fig. 2(a).

The complex crossing point is found to be

$$\tau_c = \frac{1}{2} \pm \frac{\omega_1}{2A} i . \qquad (15)$$

In order to avoid edge effects due to starting and ending the experiment at finite times it is necessary to choose $\omega_1 \ll A$, so the time integrals can be extended to $\pm \infty$. Then the dynamic and geometric contributions to the transition probability are evaluated as

$$\Gamma_d = \frac{\pi \omega_1^2}{4\delta |A|} , \qquad (16)$$

$$\Gamma_g = -\frac{\pi \omega_1^2 B}{4|A|A} . \qquad (17)$$

It will be argued that moving the detector frequency can have no physical effect in a NMR experiment, a point which is certainly true. The detector frequency serves only to define a convenient reference frame. In the present case, by choosing a different detector frame, we can even make our complex Hamiltonian look real. Does this remove the geometric component from the transition probability? Not at all. By synchronizing the detector with the rf, rather than using the frame described above, the Hamiltonian of Eq. (14) is transformed into

$$\hat{H} = 2(A - B\delta)(\tau - \tfrac{1}{2})I_z - \omega_1 I_x . \qquad (18)$$

Note the appearance of δ in the resonance offset term. In this frame, $\Gamma_g = 0$ by symmetry. When Landau-Zener theory is applied to this transformed Hamiltonian [now a valid procedure because it has the form of the Hamiltonian of Eq. (1)], the transition probability for all values of δ is obtained,

$$P = \exp \left[-\frac{\pi \omega_1^2}{4\delta |A(1 - B\delta/A)|} \right] . \qquad (19)$$

Expansion around $\delta = 0$, the adiabatic limit, yields

$$P = \prod_{n=-1}^{\infty} \exp \left[-\frac{\pi \omega_1^2}{4|A|} \left[\frac{B}{A} \right]^{n+1} \delta^n \right] , \qquad (20)$$

which shows that, even though $\Gamma_g = 0$ in this frame, the geometric component of P, $\exp[-\pi \omega_1^2 B/(4A|A|)]$, does not vanish. This expansion also gives a useful bound on where the asymptotic theory of Berry should be valid, namely, $A/(B\delta) \gg 1$.

The above analysis demonstrates that Γ_g and Γ_d are gauge-dependent quantities, that is, that their values de-
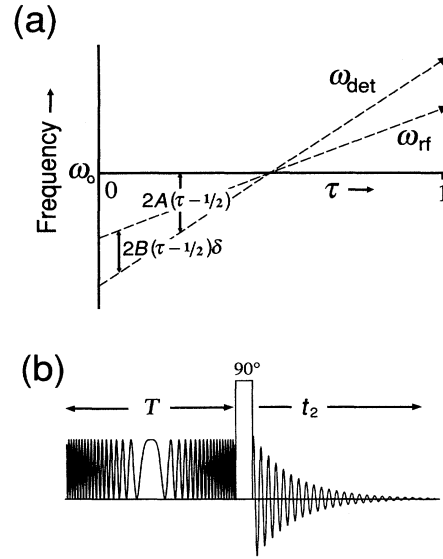

FIG. 2. (a) The transmitter and detector frequencies necessary to generate the Hamiltonian shown in Eq. (14) [Fig. 1(b)]. The detector frequency is swept linearly through resonance, to give the proper offset behavior [$\omega_0 - \omega_{det} = 2A(\tau - \tfrac{1}{2})$]; also, the rf and detector frequencies are offset by $2B(\tau - \tfrac{1}{2})\delta$, so that the phase of ω_{eff} in the xy plane is $B(\tau - \tfrac{1}{2})^2$. (b) The experimental sequence used to measure P, the nonadiabatic transition probability. First, the rf frequency sweep is applied over the time interval $[0, T]$. P is related to the resulting component of magnetization along z; this is probed with the 90° pulse, which tips it into the xy plane in the rotating frame, where it is detected in the time domain during the interval t_2. Fourier transformation to the frequency domain yields a peak whose intensity is proportional to $2P - 1$. Four such experiments, with phase-shifted probe pulses and detector frames (to cancel residual coherences and artifacts in the electronics), are coadded and integrated to yield a single data point.

pend on the basis (reference frame) in use. The original reference frame of Eq. (14) is conceptually convenient, because in it, the geometric and dynamic transition probabilities separate cleanly into Γ_g and Γ_d. The current reference frame, Eq. (18), lacks this clean separation, but is experimentally convenient. The practical signature of the lack of a clean separation in a given frame is the appearance of δ in the Hamiltonian expressed in that frame. If δ appears explicitly, then in that frame the geometry of the curve and its time parametrization are entangled, and one cannot draw conclusions about the appearance of a geometric transition probability from the shape of such a curve alone.

The existence of a real form of the Hamiltonian [Eq. (18)] is not due to any special features of the complex curve [Eq. (14)]. Any complex Hamiltonian curve can be locally transformed to a real version, to which Dykhne's theory can be applied. The resulting transition probability will be qualitatively different, however, from the usual Dykhne and Landau-Zener results, if the Hamiltonian

curve in a δ-independent frame is both complex and sufficiently asymmetric. The new feature in P is, of course, the δ-independent component (expΓ_g in a δ-independent basis). The fact that Γ_g vanishes in some frames but P retains its δ-independent factor is the analog of the removability of Berry's phase, that is, the fact that Berry's phase can always be locally transformed away but nevertheless observables still show the underlying geometry of the system.[26] This freedom of choice of basis is a manifestation of the gauge invariance of P. We take advantage of this freedom by measuring P in the frame of Eq. (18), and analyzing the data in the frame of Eq. (14), for easier comparison with Berry's results.

B. Measurement of P

The Zeeman resonance in carbon-13-enriched carbon disulfide provided the two-level system for our experiments. We used an 11.7-T magnet, corresponding to a ^{13}C resonance frequency of 125.6 MHz; the static magnetic field was shimmed to give a line of full width at half maximum of 15 Hz.[27] The NMR spectrum of this sample consists of a single sharp line since most (99%) of the spin-$\frac{1}{2}$ ^{13}C is bonded to spin-0 sulfur. The longitudinal relaxation time (T_1) for our sample was 22 seconds, which defines the time scale for rapid passage experiments: they must be short compared to T_1. All results presented below were acquired with sweep times ≤ 0.6 sec. The data were collected on a Chemagnetics CMX-500 NMR spectrometer, using a Sciteq direct digital synthesizer for control of the detector and rf frequencies.

Measuring P amounts to measuring the diagonal elements of the density matrix. The initial density matrix in our experiment is essentially I_z (Refs. 24 and 25); after subjecting this to a rf sweep, the component remaining along the z axis is proportional to $2P-1$. A 90° pulse following the sweep brings this component to the xy plane in the rotating frame, where it can be detected in the time domain. The entire measuring procedure is shown schematically in Fig. 2(b). A standard cyclically ordered phase sequence (CYCLOPS) phase cycle is applied to the 90° pulse and detector, to remove residual coherences and hardware imperfections.[28] The (signed) area of the peak in the frequency domain S is proportional to $2P-1$, and is normalized to the signal from a very slow (adiabatic) sweep, $S_{\max}$, for which $P=0$. Thus P is extracted from the measured peak areas as $P=\frac{1}{2}(1-S/S_{\max})$.

IV. RESULTS

We demonstrate generation of the Hamiltonian of Eq. (14) by showing, in Fig. 3, the response of the sample magnetization to it, for $\delta=1.66$ sec^{-1} ($A/B\delta=18.9$), that is, nearly adiabatic evolution. For such a case, the magnetization vector tracks the direction of the Hamiltonian vector shown in Fig. 1(b) and gives a direct picture of the geometry of the Hamiltonian curve.

Measurement of Γ_g requires nonadiabatic traversal of the Hamiltonian curve, for which the magnetization no longer keeps up with the Hamiltonian. We take advan-
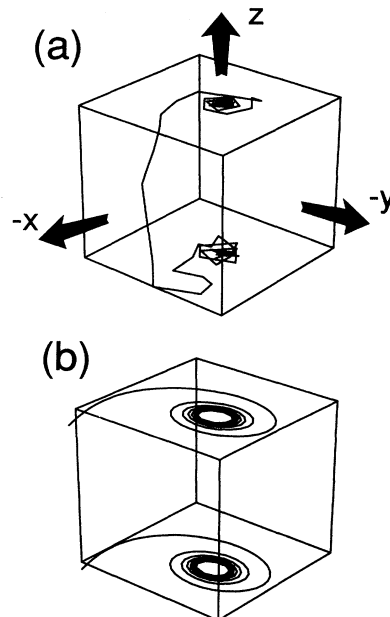

FIG. 3. (a) Response of the sample magnetization to the Hamiltonian of Eq. (14) [Fig. 1(b)], in the adiabatic regime. This experiment was performed with an interrupted version of the sequence described in Fig. 2(a), in which both the phase and amplitude of the magnetization were measured at points during a single sweep, rather than just at the end of a sweep. For adiabatic evolution the magnetization tracks the Hamiltonian curve shown in Fig. 1(b), as is seen here, though the length of the magnetization vector is conserved and so lies on the surface of a sphere, rather than a cylinder. (b) For clarity, an expanded (and truncated) theoretical curve of the magnetization is shown.

tage of the fact that we have an expression for P valid for all δ, by fitting the theory to our measurements of P over a range of sweep times. The results are shown in Fig. 4. The experimental parameters are $A=50$ kHz, $B=\pm5,000$ rad, and $\omega_1=393$ Hz. Determination of these parameters is discussed below. Changing the sign of B is equivalent to the transformation $H(\tau)\rightarrow H(-\tau)$, that is, time reversal.[4] Close agreement between the exact theory, Eq. (19), and experiment is obtained over the full range of δ. We have performed the same experiment with different values of $|B|$ and ω_1, and the graphs of P (not shown) scale according to Eq. (19).

V. DISCUSSION

A. Determination of Γ_g

Using the data shown in Fig. 4 we can extract the geometric contribution to P in two ways.[4] First we plot $\ln(1/P)$ versus $1/\delta$, that is, versus sweep time—in the nearly adiabatic regime, such a plot should be linear, with slope $\delta\Gamma_d$ and intercept $-\Gamma_g$. The nonzero intercept reflects the fact that the geometric component persists into the adiabatic limit, although $P\rightarrow0$ in this limit so it cannot be measured there. The data are plotted this way in Fig. 5(a), and three regimes can be identified. At short
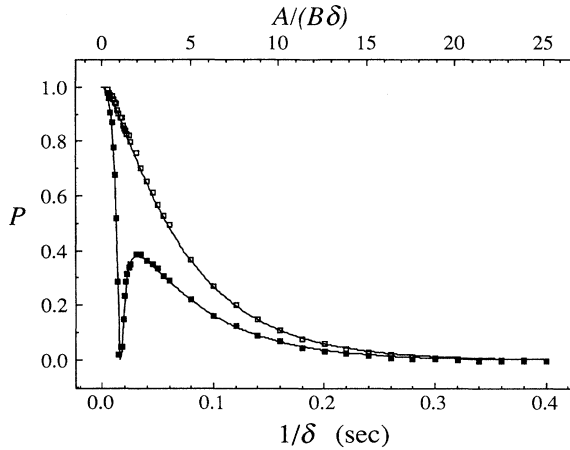
FIG. 4. The nonadiabatic transition probability, measured as a function of adiabaticity parameter for the Hamiltonian of Eq. (14). Parameters are $A = 50$ kHz, $B = \pm 5000$ rad, and $\omega_1 = 393$ Hz. Changing the sign of B amounts to traversing the curve in time-reversed fashion. The filled squares are for $B = +5000$ rad, and the open squares for $B = -5000$ rad. The solid curves show the theory for this case, Eq. (19), which is exact, describing both the adiabatic and nonadiabatic limits. $A/(B\delta)$, shown on the top axis, is a dimensionless adiabaticity parameter (see text), which scales out the specific values of the constants used in the experiment.
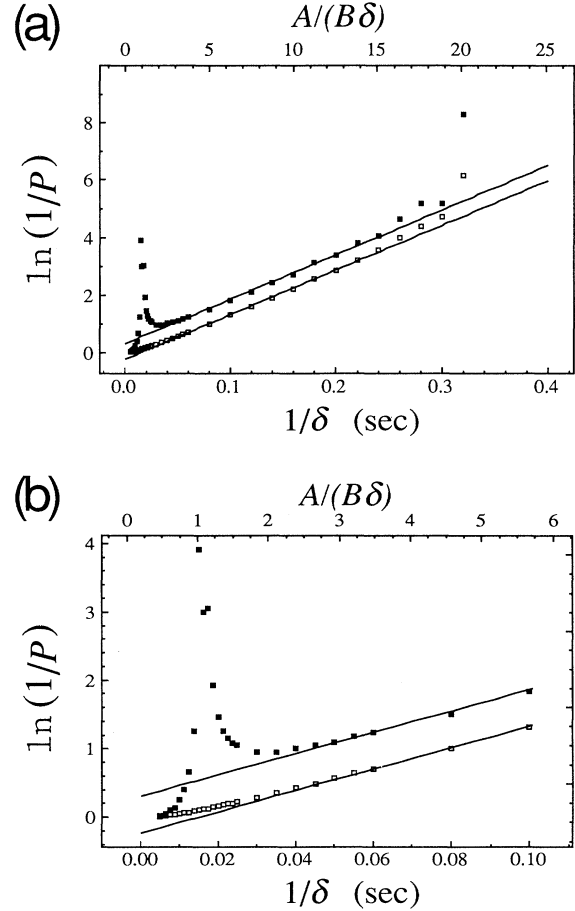

FIG. 5. (a) The same data as shown in Fig. 4, now plotted as $\ln(1/P)$ vs $1/\delta$ in order to extract the geometric transition probability. Three regimes, as discussed in the text, can be identified. At small values of $1/\delta$ the dynamics are strongly nonadiabatic, and the asymptotic theory of Berry is not valid here. For large $1/\delta$, the adiabatic limit, P is too small to measure accurately in our experiment, as is evidenced by the increased scatter in the data at long sweep times. The intermediate regime, however, is accessible to experiment and is described by Berry's theory. This regime requires $A/B\delta \gg 1$ [see Eq. (20)]; we see that experimentally $A/B\delta \gtrsim 4$ appears to be sufficient. The figure also shows the theory of Berry, which appears as straight lines of slope $\delta\Gamma_d = 15.3$ sec^{-1} and intercept $\Gamma_g = \pm 0.243$. The sign change in Γ_g is due to its behavior under time reversal. The intercepts are shown more clearly in (b), which also shows the behavior for small $1/\delta$; both experimental curves go to zero here, since $P \to 1$ in this limit.

sweep times the data are nonlinear, as expected—the asymptotic theory should not apply here. Also, at the shortest times, $P \to 1$, and $\ln(1/P) \to 0$ as shown in Fig. 5(b). At very long times, $P \approx 0$, and we cannot measure it accurately due to our signal-to-noise constraints. The intermediate regime, however, shows the expected linear behavior, with offset. Equation (20) shows that Berry's theory should hold, for the present Hamiltonian, when $A/B\delta \gg 1$. The data show linearity for $A/B\delta \gtrsim 4$; theoretical requirements for adiabatic evolution are frequently harsher than those encountered experimentally. Finally, note that the intercepts in Fig. 4 are positive and negative, as B is changed in sign; this is due to the fact that Γ_g changes sign under time reversal, but Γ_d does not.[4]

Berry's theory predicts, for the values of A, B, and ω_1 listed above, that $|\Gamma_g| = 0.243$ and $\delta\Gamma_d = 15.3$ sec^{-1}. These lines are plotted in Fig. 5. Least-squares fits to our data give $\Gamma_g = 0.26$ and $\delta\Gamma_d = 16$ sec^{-1} for $B = -5000$ rad, and $\Gamma_g = -0.23$, $\delta\Gamma_d = 15$ sec^{-1} for $B = +5000$ rad. Quantitative agreement, while not perfect, is reasonable, given the amplification of errors at small P introduced by the logarithmic plot and the difficulty of measuring ω_1, the amplitude of the rf field, precisely in our apparatus; we comment on this difficulty below.

The above-stated time-reversal behavior affords a second way to extract Γ_g. Plotting $\frac{1}{2}\ln(P_{B>0}/P_{B<0})$ versus sweep time should give a line of zero slope with intercept Γ_g; the data plotted this way are shown in Fig. 6. This determination yields $\Gamma_g = -0.26 \pm 0.01$, to be compared with the theoretical value of $\Gamma_g = -0.243$. The

same three regimes observed in Fig. 5 can be identified, as $1/\delta$ changes from small to large values.

B. Behavior with respect to time reversal

In Sec. V A we used the behavior of P under time-reversal to extract Γ_g. Near the adiabatic limit, where the asymptotic theory is valid, this behavior is expressed simply by the sign change in Γ_g. Figure 4 shows that,
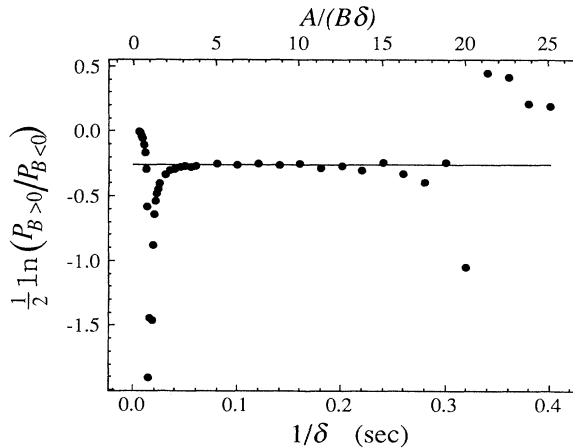
FIG. 6. The data of Fig. 4, plotted as $\frac{1}{2}\ln(P_{B>0}/P_{B<0})$ vs $1/\delta$. Due to the behavior under time reversal, Γ_g adds while Γ_d cancels; the asymptotic theory thus predicts a line of slope zero and intercept Γ_g for this plot. The theory is confirmed, and the same three regions of Fig. 5 can be identified.

farther from this limit, the behavior of P for $B>0$ differs qualitatively from that for $B<0$: for $B>0$ an inversion notch is observed, where $P \rightarrow 0$, even though $B\delta/A$ is not small, while no such notch is observed for $B<0$. Though this feature occurs outside the regime of validity of Berry's asymptotic theory, its sensitivity to time reversal and the fact that no such behavior occurs in the conventional Landau-Zener Hamiltonian [Eq. (1)] merit attention.

We first consider how the rf frequency depends on the sweep time $1/\delta$. As discussed above, the shape of the Hamiltonian curve of Fig. 1(b) will be independent of the sweep rate for fixed parameters A and B. However, the situation is quite different in the frame defined by the rf [Eq. (18)]: Fig. 2(a) indicates that the rf field sweeps through a total range of $2(A-B\delta)$ as it crosses the Larmor frequency. For $B>0$, the range is swept from negative to positive offsets for small δ, and positive to negative for large δ; when $\delta = A/B$, the range is not swept at all. For $B<0$, all sweeps are negative to positive. Physically, $\delta = A/B$ "sweeps" correspond to continuous resonant irradiation. This condition represents a pathological solution to the Landau-Zener problem, in that P becomes an oscillatory function of time at this point. Experimentally, this pathology is easy to avoid, because it is very narrow: the transition occurs while the resonance offset is in a range around zero of order ω_1. Thus the data of Fig. 4 near the notch satisfy the condition that the initial and final resonance offsets are large on the scale of the transition itself, so for these points one may still think in terms of an inversion of the magnetization. The reason that the inversion becomes nearly perfect here, even though $A/B\delta \approx 1$, is that the rate of change of the sweeping field, compared to the effective field strength, is very small. Thus while ω_{eff} is in the transition region it changes slowly, and adiabatic behavior is observed.

It is also instructive to consider the origin of the notch

in the frame of Eq. (14), that is, the frame of Fig. 1(b). In this frame the curves corresponding to the two signs of B can be derived from each other by inversion through the origin, the main effect of which is to reverse their helicities. Thus for $B>0$, the helicity is decreasingly positive as the crossing is approached, and increasingly negative afterwards, while the opposite holds for $B<0$. As is well known from conventional NMR theory, only one sense of circularly polarized irradiation can effect a transition, that sense being defined relative to the sign of the applied static field.[24,25] Therefore, we expect transitions when the sense and rate of helicity are properly correlated with swept resonance offsets as defined by the detector frame. This immediately explains why the notch appears only for $B>0$. Furthermore, the spin inversion to which the notch corresponds appears here as a rather intricate spin trajectory, quite unlike the smooth adiabatic inversion of the conventional Landau-Zener picture [Eq. (18)].

In the context of the helical Hamiltonian, the crossing point when $A/B\delta \approx 1$ is decidedly nonadiabatic. This is acceptable: the description of a transition as adiabatic is frame dependent. We see that by viewing the Hamiltonian of Eq. (14) as a simple Landau-Zener problem, by using the frame of Eq. (18), we arrive at a simple picture of the inversion process, for which, however, the geometrical component of the transition probability comes out only after a complete analysis. In the original frame, the geometry is evident, but a description of the transition itself becomes more difficult. Each frame has advantages, and of course the same result is obtained for P in either case.

C. Determination of ω_1

The results shown above provide a simple determination of the geometric component of the transition probability. We encountered one difficulty in making the measurements, which we now discuss in some detail. The various expressions for P, whether exact or asymptotic, are quite sensitive to ω_1, the rf field amplitude, as they depend exponentially on ω_1^2. The other parameters in these expressions, A and B, are offsets that are programmed into the digital synthesizer and hence are known. ω_1 must be measured independently, however. Such a measurement is typically accomplished by determining the length of time needed for a 360° pulse on resonance, t_{360}, because $\omega_1 t_{360} = 2\pi$. We found that our data could be fit precisely by the theory only when the value of ω_1 used in the formulas for P was adjusted to a lower value from the value given by $2\pi/t_{360}$, typically about 10% lower. This discrepancy does not seriously undermine our confidence in our test of the theory, however, primarily because of Fig. 4. In this figure P is plotted for a wide range of δ, and should be fit by Eq. (19). By using a nonlinear least-squares fitting procedure with this formula, and ω_1 as the only adjustable parameter, very good agreement with the data is obtained. The goodness of fit suggests that ω_1 as obtained from t_{360} is slightly high, but that other features of the experiment work as expected, because the functional form for P agrees closely with the theory. We describe below several possible mechanisms that might ac-

count for this discrepancy in the value of ω_1.

One likely source of error is homogeneity in the magnetic fields. There are two possibilities: inhomogeneity in the static field and in the rf field. We rule out the former as a source of error, because experiments carried out with a range of shim settings, corresponding to resonance linewidths ranging from 2 to 30 Hz, gave no change in the discrepancy in ω_1 values. This is not surprising, since in our experiments the initial and final resonance offsets are much greater than this small spread in ω_0. Thus all spins in the system will be affected equally by the sweep, though possibly at slightly different times during the sweep.

We now turn to rf inhomogeneity. The data shown in this paper were obtained with a solenoidal coil for rf excitation and detection, which was about the same size as our sample. The coil was inclined at an angle, and since the sample did not completely fill its container, a nonsymmetric distribution of sample with respect to the coil resulted. We can expect such a nonuniform distribution to exacerbate the effects of the inhomogeneity inherent in the coil. The observable consequence of rf inhomogeneity is to give a distribution of ω_1, rather than a single value. We were able to measure this distribution approximately, and average the theory with respect to it; this procedure does not significantly change the functional form predicted for P, and could account for 10–30% of the discrepancy in ω_1 values.

Radiation damping, that is, secondary effects due to the reradiation of the rf field generated in the coil by the relaxing magnetization,[24] is another possible source of error. This mechanism has already been considered in the context of ARP experiments.[29,30] Numerical integration of the Bloch equations in the presence of a small (3 Hz) amount of radiation damping shows that the form of the graph of P is essentially unchanged, but is shifted to an effective value of ω_1 about 3% smaller than the nominal value. Thus the correction is in the same direction as our observed discrepancy, but it is likely that the amount of radiation damping present in our system is substantially less than 3 Hz.

Other possible sources of error are the digital generation of the frequency sweeps, and the changing probe response as a function of resonance offset. We were able to show experimentally and by simulation that the number of digitization steps we used (1792) was sufficiently large to leave the results unaffected, and that the relatively low probe Q of 230 yielded a flat response within 2% over the frequency range used.

While we could not quantitatively account for the entire difference between the independent measurement of ω_1 and the fit to measured values of P, rf inhomogeneity seems the most likely mechanism to cause the observed discrepancy. This conjecture could be checked by performing a more quantitative independent measurement of the coil characteristics than we were able to, or possibly by using a very small, symmetrically constructed sample

container. As an aside, we remark that this experiment, with its sensitivity to ω_1, might provide a very precise way to calibrate small rf field strengths in other NMR measurements.

VI. CONCLUSIONS

We have provided the first experimental study of the geometric transition probability recently described by Berry.[4] Various features of the theory were tested, including the independence of the geometric factor to the rate of change of the Hamiltonian; the theory is confirmed in all respects.

We anticipate that the geometric transition probability will prove to be an important consideration in a wide variety of experiments. Observing the probability is quite straightforward—no complicated interference experiments are necessary, nor are closed loops in parameter space needed, as they are in the case of Berry's phase, for unambiguous determination. In chemical physics, Landau-Zener treatments are frequently used in the study of scattering and dissociation processes; when fields or other mechanisms which break time-reversal symmetry are present, we expect that the geometric term will play a role.

A simple extension of this work is a modification of the experiment used to generate the data shown in Fig. 3, to measure the population change as a function of τ *during* the sweep—a simple formula for this is derived in another recent paper by Berry.[31] Work along these lines is currently underway in our laboratories.

At this point an important theoretical problem is to extend the treatment of Berry to the case of multiple avoided crossings. This has been considered for real Hamiltonians by Pechukas and co-workers,[20,21] and the difficulties increase much faster than the number of avoided crossings (degeneracies in the complex time plane). The effect of multiple degeneracies is not simply additive. Such problems will also apply to the geometric case, but must be addressed in order to apply the theory to many realistic molecular systems. A general geometric framework for Γ_g, analogous to the type developed by Simon for Berry's phase,[32] could be helpful here, but it is not clear to us how to develop one for open paths parametrized by complex time.

[1] A. Shapere and F. Wilczek, *Geometric Phases in Physics* (World Scientific, Singapore, 1989).

[2] J. W. Zwanziger, M. Koenig, and A. Pines, Ann. Rev. Phys. Chem. **41**, 601 (1990).

[3] M. V. Berry, Proc. R. Soc. London Ser. A **392**, 45 (1984).

[4] M. V. Berry, Proc. R. Soc. London Ser. A **430**, 405 (1990).

[5] M. V. Berry, Proc. R. Soc. London Ser. A **414**, 31 (1987).

[6] Y. Aharonov and J. Anandan, Phys. Rev. Lett. **58**, 1593 (1987).

[7] J. Anandan, Phys. Lett. A **133**, 171 (1988).

[8] N. Datta, G. Ghosh, and M. H. Engineer, Phys. Rev. A **40**, 526 (1989).

[9] B. Zygelman, Phys. Rev. Lett. **64**, 256 (1990).

[10] J. Samuel and R. Bhandari, Phys. Rev. Lett. **60**, 2339 (1988).

[11] J. C. Garrison and E. M. Wright, Phys. Lett. A **128**, 177 (1988).

[12] S. -I. Chu, Z. -C. Wu, and E. Layton, Chem. Phys. Lett. **157**, 151 (1989).

[13] J. Anandan and A. Pines, Phys. Lett. A **141**, 335 (1989).

[14] P. V. Coveney, D. S. F. Crothers, and J. H. Macek, J. Phys. B **21**, L165 (1988).

[15] E. A. Solov'ev, in *Topological Phases in Quantum Theory,* edited by B. Markovski and S. I. Vinitsky (World Scientific, Singapore, 1989).

[16] J. Moody, A. Shapere, and F. Wilczek, *Geometric Phases in Physics* (Ref. 1), p. 160.

[17] N. Rosen and C. Zener, Phys. Rev. **40**, 502 (1932).

[18] C. Zener, Proc. R. Soc. London **137**, 696 (1932).

[19] A. M. Dykhne, Zh. Eksp. Teor. Fiz. **41**, 1324 (1961) [Sov. Phys.—JETP **14**, 941 (1962)].

[20] J. P. Davis and P. Pechukas, J. Chem. Phys. **64**, 3129 (1976).

[21] J. -T. Hwang and P. Pechukas, J. Chem. Phys. **67**, 4640 (1977).

[22] P. Pechukas, T. F. George, K. Morokuma, F. J. McLafferty, and J. R. Laing, J. Chem. Phys. **64**, 1099 (1976).

[23] A. Messiah, *Quantum Mechanics* (Wiley, New York, 1958).

[24] A. Abragam, *Principles of Nuclear Magnetism* (Oxford, Oxford, 1962).

[25] C. P. Slichter, *Principles of Magnetic Resonance,* 3rd ed. (Springer, New York, 1989).

[26] G. Giavarini, E. Gozzi, D. Rohrlich, and W. D. Thacker, J. Phys. A **22**, 3513 (1989).

[27] This linewidth is due almost entirely to inhomogeneity in the static magnetic field.

[28] D. I. Hoult and R. E. Richards, Proc. R. Soc. London Ser. A **344**, 311 (1975).

[29] M. Odehnal and V. Petricek, Phys. Lett. A **41**, 359 (1972).

[30] W. S. Warren, S. L. Hammes, and J. L. Bates, J. Chem. Phys. **91**, 5895 (1989).

[31] M. V. Berry, Proc. R. Soc. London Ser. A **429**, 61 (1990).

[32] B. Simon, Phys. Rev. Lett. **51**, 2167 (1983).